*Biogeochemistry* **55:** 311–325, 2001.


# Residual phosphorus in runoff from successional forest on abandoned agricultural land: 2. Hydrological and soluble reactive P Budgets

CHRISTOPHER A. SCOTT[1] & MICHAEL F. WALTER[2]
[1]*India Regional Office, International Water Management Institute, c/o ICRISAT, Patancheru, A.P. 502-324, India;* [2]*Dept. Agricultural & Biological Engineering, Cornell University, Ithaca NY 14853 U.S.A.*

**Key words:** forest succession, hydrology, modeling, phosphorus

**Abstract.** Residual P from historical farm practices has been linked to elevated soluble reactive phosphorus (SRP) transport in runoff from a field study site in the Catskills Mountains, New York, U.S.A., with a P source assay indicating that successional forest floor biomass was the major contributor to runoff SRP. In this paper, we assemble hydrological and SRP budgets that indicate net SRP loss of 0.123 kg $ha^{-1}$ $yr^{-1}$ occurs from the site (composed of 0.044 kg $ha^{-1}$ $yr^{-1}$ precipitation input, with 0.143 kg $ha^{-1}$ $yr^{-1}$ and 0.024 kg $ha^{-1}$ $yr^{-1}$ losses in runoff and groundwater, respectively). These findings contrast with conservative P cycling reported for undisturbed forests. Coupled hydrological and SRP data are analyzed suggesting that catchment ambient and equilibrium SRP concentrations corresponding to groundwater and long-term average runoff concentrations are in the range capable of contributing to eutrophication of receiving waters. A physically based variable source area hydrological model is tested to simulate SRP export using deterministic concentrations. The three-layer model (surface runoff, shallow lateral flow, and groundwater) is parameterized using spatially distributed data from additional P source assays and field hydrological monitoring for the site. Differences in simulated and observed outflow and SRP export are partially explained by forest evapotranspiration and frozen soil processes. The field data, SRP budgets and simulations show that sufficient residual P pools exist to prolong net SRP loss rates until ecosystem processes re-establish more conservative P cycling.

## Introduction

Part 1 of this paper (Scott et al. 2001) demonstrated that coupled biogeochemical and hydrological processes provided the best explanation for elevated soluble reactive phosphorus (SRP) in runoff from an old-field successional forest stand in the Catskills Mountains, New York, U.S.A. Flow-weighted annual $SRP_{mean}$ of 0.0127 mg $L^{-1}$, linked to residual P in regrowth forest

*Table 1.* Physical and chemical properties of field site soils

| | | Series | | |
|---|---|---|---|---|
| | | Halcott-Mongaup-Vly | Elka-Vly complex | Lewbeach |
| Texture | Units | Channery silt loam, very rocky | Channery loam | Channery loam, very strong |
| Area | ha | 2.3 | 7.9 | 6.4 |
| Depth to bedrock | cm | 38 | 150 | 38 |
| Slope | % | 0–22 | 9–35 | 0–33 |
| $\theta_{saturation}$ | | 0.22 | 0.46 | 0.26 |
| $\theta_{fieldcapacity}$ | | 0.18 | 0.22 | 0.21 |
| $\theta_{available}$ | | 0.04 | 0.24 | 0.05 |
| Rock content | | 0.58 | 0.20 | 0.55 |
| $P_{available}$ | mg $kg^{-1}$ | 1.774 | 1.342 | 1.841 |
| pH | | 4.88 | 4.84 | 5.36 |
| Organic matter | % | 6.5 | 5.1 | 5.9 |
| $Fe_{available}$ | mg $kg^{-1}$ | 42.2 | 39.9 | 14.9 |
| $Al_{available}$ | mg $kg^{-1}$ | 181.2 | 151.6 | 122.4 |

biomass, was found to be in the range capable of contributing to the eutrophication of receiving waters.

For the same field site, the objectives of this – part 2 of the paper – are to: (a) assess hydrological transport mechanisms, (b) determine net annual SRP fluxes through the construction of hydrological and SRP mass balances, and (c) parameterize and run a physically-based hydrological model to simulate SRP export. Only data or findings pertinent to the analysis presented here are repeated from part 1.

## Methods and materials

The soils at the site, derived from glacial till and acid sandstone and shale parent material, are coarse, loamy, mixed, frigid, lithic dystrochrepts of the Halcott-Mongaup-Vly, Elka-Vly complex, and Lewbeach series with the characteristics presented in Table 1. Physical properties are as reported in the STATSGO database. Available moisture content, $\theta_{available}$, is defined as $\theta_{saturation}$-$\theta_{fieldcapacity}$. Available nutrients and minerals (P, Fe, Al) were determined using standard New York State methods – Morgans's solution extraction (10% sodium acetate in 3% acetic acid buffered to pH 4.8, using a 1:5 w/v soil:solution ratio; Morgan 1941). Available P was measured colorimetrically by stannous chloride reduction; $Fe_{available}$ and $Al_{available}$ were measured by atomic absorption.

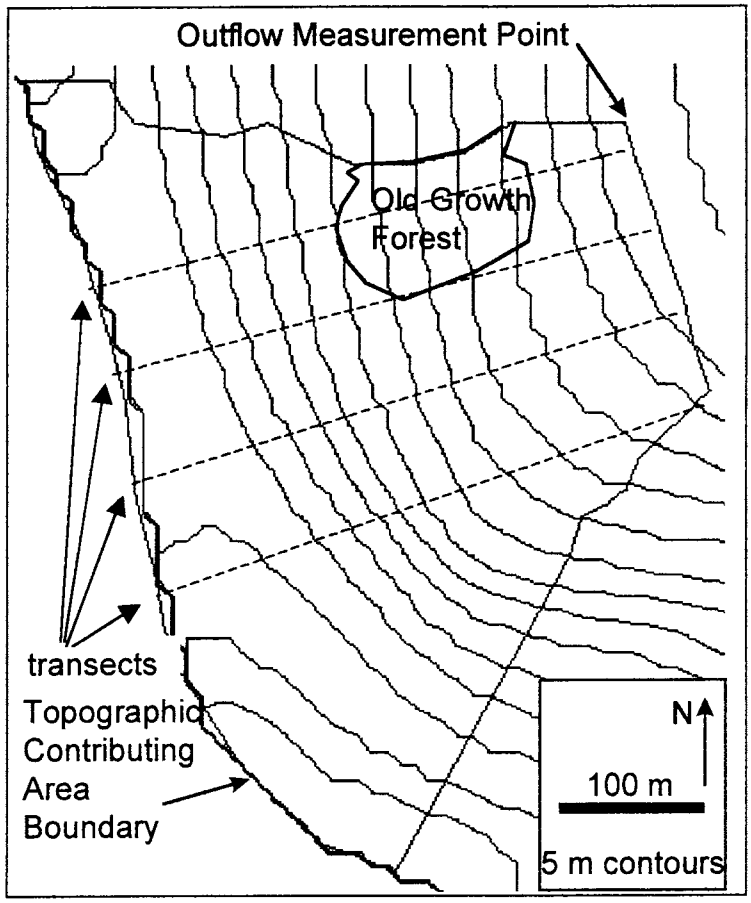


*Figure 1.* Study site showing transects for P source material assay.

An additional P source material assay was conducted at the site on 10 September 1997. Organic material from the surface litter layer 0–5 cm deep and mineral soil at 15–20 cm depth were collected at approximately 30 m spacing along four parallel transects running from the outflow drainage ditch upslope to the ridge top defining the catchment (Figure 1). The spacing between adjacent transects was approximately 60 m. A total of 94 (46 litter, 48 soil) samples were analyzed for Morgan available P.

Distribution (desorption-partition) coefficients $K_d$ based on Morgan's solution were developed separately for litter and soil by measuring sorbed and solution concentrations after 72 hr of complete mixing. For organic matter, $K_{d,litter}$ was derived as 4238.5 L $kg^{-1}$. For mineral soil, $K_{d,soil}$ was derived as 143.8 L $kg^{-1}$ (Scott 1998a).

Surface runoff and shallow lateral flow (collectively treated as runoff throughout this paper) were collected at the site in a surface diversion ditch excavated (in 1993) approximately 1.5 m deep down to the impermeable layer. Runoff at the site was gauged using an H-flume installed in a propane-heated, insulated box (for instrumentation details, see Scott 1998a; Scott 1998b). Ice build up during the winter was freed on a regular basis. Eight calibrations at different discharges using a stopwatch and graduated cylinder matched gauged flow within 11%. Loss under the flume headwalls (installed 30 cm into the fragipan and grouted with hydraulic cement and bentonite) was estimated to be less than 1 L $s^{-1}$ when head increases during peak discharge ($<$ 5% of Q). Runoff from the old growth forest could not be isolated, as upslope water flowed through this area.

Multiple runoff samples were collected at variable intervals during runoff events using an ISCO® automatic sampler. During periods of relatively constant discharge, single grab samples were collected. 'Events' were defined operationally on the basis of weather forecasts when flow was anticipated to rise significantly. Runoff discharge, precipitation, and solar radiation were logged on a 15 min interval. Air temperature, soil temperature (at 10 cm and 20 cm depth) were recorded at a separate location 960 m from the forest site, also on a 15 min interval. Snow depth and density and soil freezing were recorded at seven locations within the forest stand on 21 separate occasions during the winter of 1996–1997.

Hydrological simulation was performed using the Cornell Soil Moisture Routing (CSMR) model, a distributed parameter model in GRASS, run on 10 m resolution and a daily time step. CSMR was designed to predict saturated areas by routing moisture through the landscape (Frankenberger et al. 1999; Zollweg et al. 1996) based on the variable source hydrological processes first described by Hewlett & Nutter (1970) and Dunne & Black (1970). Model outputs for daily surface runoff (including its spatial distribution with relation to litter P sources as established by the assay), shallow lateral flow, and groundwater flow were generated. The interpolated surface of available P was generated in GRASS using numerical approximation based on weighted averaging techniques.

## Results and discussion

### *Phosphorus transport hydrology*

Scott et al. (2001) showed that regrowth biomass has the characteristics most likely to account for the 0.0127 mg $L^{-1}$ $SRP_{mean}$ annual concentration observed at the site. Hydrological mechanisms must exist for dissolution

and transport of SRP to the outflow measurement point. In this section, we analyze the flow and concentration data to explore causes for the elevated concentrations.

'*Ambient*' and '*equilibrium*' SRP concentrations, for zero runoff discharge Q and constant Q respectively, produced results comparable to the 0.0127 mg $L^{-1}$ $SRP_{mean}$. Ambient SRP was derived through regression of SRP and Q, in order to explore whether SRP concentrations can be explained by dilution of source P. This yielded the relationship:

$$SRP = 0.0008Q + 0.0138 \quad (1)$$

which is significant at $p < 0.01$ ($n = 133$). The 0.0138 mg $L^{-1}$ intercept representing ambient SRP at zero discharge compares well with the observed $SRP_{mean}$. With diminishing flow, runoff is increasingly comprised of shallow groundwater that should have SRP concentration at equilibrium with sorbed P in the mineral soil horizon. This is corroborated by laboratory work that established 143.8 L $kg^{-1}$ as the value of $K_d$, the distribution (desorption-partition) coefficient based on Morgan's solution extraction. Assuming equilibrium linearity, ambient concentration, $C_a$, is determined from sorbed concentration, S, by:

$$C_a = \frac{S}{K_d} \quad (2)$$

Taking S as the average of the three $P_{available}$ values reported in Table 1 yields $C_a = 0.0115$ mg $L^{-1}$ which is somewhat lower but compares favorably with the 0.0138 mg $L^{-1}$ ambient concentration derived through regression analysis in Equation 1.

Equation 1 indicates that a proportional relationship exists between SRP and Q, indicating that simple dilution processes cannot explain SRP concentrations. A similar, positively correlated relationship between event SRP and Q was found for manured pastureland in the same study area (Scott 1998a). Rekolainen (1989) observed similar trends particularly on agricultural land.

The positive SRP vs. Q trend has at least two possible, inter-related interpretations. First, runoff of higher velocity and turbulence selectively entrains organic matter and fine clay fractions which are the primary source of SRP in runoff from the site. Given that variable source processes dominate Catskills hydrology (Frankenburger et al. 1999), runoff occurs after the soil surface transiently becomes saturated. As a result, P source material at or near the soil surface is dissolved or entrained in runoff for subsequent transport to the outflow. Second, the surface area and duration of contact between runoff water and mineral soil or bed sediments in surface flowpaths (both capable of re-adsorbing SRP) are reduced with increasing discharge.

A separate indicator, related to ambient concentration and producing a result comparable to observed $SRP_{mean}$, is the '*equilibrium*' concentration, or SRP concentration for constant flow. This was derived for the catchment by regression of daily SRP vs. *dQ/dt*, the time derivative of discharge. Time series SRP(t) were recalculated to yield daily mean SRP for multiple-day events, producing the following positive correlation:

$$\mathrm{SRP} = 0.0014[dQ/dt] + 0.0130 \tag{3}$$

Equation 3 is significant at $p < 0.10$ because a reduction in sample size (n = 39) was necessary given that the differentiation interval $dt$ = 1 d encompassed numerous data points per event. At constant flow, the steady state concentration generated by the catchment was 0.0130 mg $L^{-1}$, compared to $SRP_{mean}$ of 0.0127 mg $L^{-1}$. Interpretation of the equilibrium value is best illustrated not by considering daily or monthly fluctuations in Q (where clearly *dQ/dt* $\neq$ 0), but rather yearly Q fluctuations, which may be assumed to be zero. Consequently, the equilibrium concentration is linked to the longer-term average catchment concentration, which incorporates fluctuations in both ambient (groundwater) and dynamic (surface water) concentrations during events.

The slope in Equation 3 indicates that SRP increases with increasing Q, as illustrated by the following example based on variable source area dynamics. The slope gives a 0.0014 mg $L^{-1}$ increase in SRP per unit L $s^{-1}$ $d^{-1}$ increase in Q (equal to 0.01 mg $L^{-1}$ per 7.14 L $s^{-1}$ $d^{-1}$). Based on the 16.6 ha topographic contributing area (the maximum possible value for the actual contributing area during any individual event), this converts to a 0.01 mg $L^{-1}$ SRP increase resulting from runoff of 4 mm $d^{-1}$. For illustration, the 15–16 April 1996 event had 28.5 mm $d^{-1}$ of precipitation (on a saturated area flagged out and later transit-surveyed as 3.2 ha, or 19% of the topographic contributing area). The event runoff, therefore, represented a 5.5 mm $d^{-1}$ (19% of 28.5 mm $d^{-1}$) increase over the previous day, assuming no change in moisture storage (which is reasonable based on the observation that 34.5 mm precipitation had fallen on the preceding two days). From the SRP vs. *dQ/dt* regression, the 5.5 mm $d^{-1}$ Q increase would be predicted to cause a 0.0147 mg $L^{-1}$ increase in SRP over the equilibrium concentration of 0.0130 mg $L^{-1}$ derived from the regression, yielding a predicted daily concentration of 0.0277 mg $L^{-1}$. The observed daily SRP concentration was 0.0296 mg $L^{-1}$ for this event, which corroborates Equation 3 and shows that SRP is positively correlated with *dQ/dt*.

To explore the contention that solute concentrations in runoff (to be distinguished from the runoff water itself) primarily reflects surface P sources transported by precipitation ('new') water as opposed to profile-derived

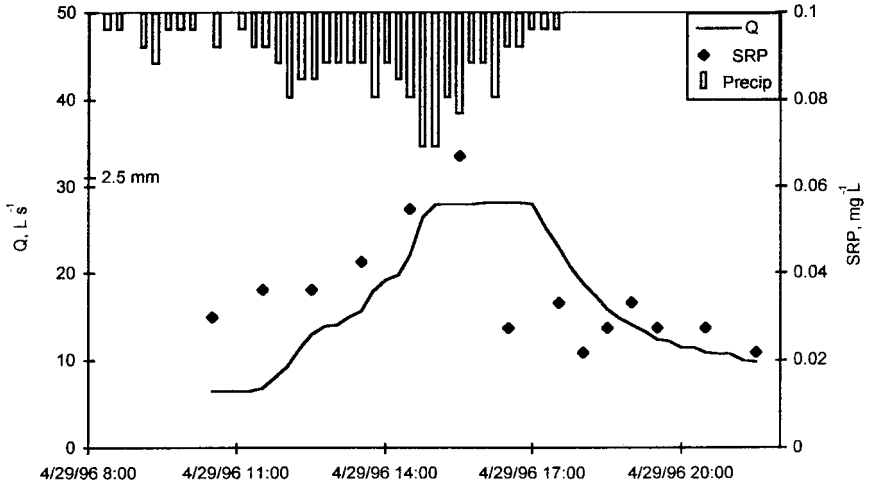


*Figure 2.* April 29, 1996 event hydrograph and SRP time series with coinciding SRP, discharge and precipitation peaks.

solutes in soil water, we analyzed the runoff and SRP time series for the 29 April event shown in Figure 2. SRP rose with Q, with several dilutions resulting from precipitation peaks, notably at 13:30 and at 15:00. The catchment reached its maximum area of saturation after 15:00 when SRP peaked; subsequently, SRP and Q declined simultaneously with precipitation. Similar responses are described for dissolved organic carbon (Boyer et al. 1997). If soil profile sources transported by soil water were the primary contributors to the SRP signal at the outflow, SRP concentrations would have remained elevated well into the hydrograph recession as saturated soils drained. Instead, the SRP, Q, and precipitation peaks all coincided, supporting the argument that SRP transported in runoff is primarily precipitation-driven and reflects soil surface conditions.

*Hydrological mass balance*

Hydrological processes were assumed to transport all P inputs and losses from the site (timber removal was not observed during the period of field monitoring). As a precursor to an SRP budget, we constructed a hydrologic mass balance. For flows, the balance was based on daily total precipitation and runoff recorded throughout the monitoring period. Groundwater flux ($Q_g$), separated into deep ($Q_d$) and shallow ($Q_s$) components, was calculated as the residual term in the mass balance:

$$Q_g(t) = Q_d(t) + Q_s(t) = Q_p(t) - Q_r(t) - Q_e(t) \quad (4)$$

where $Q_p$ is precipitation, $Q_r$ is runoff, and $Q_e$ is ET loss – calculated following Hamon (1961) and Jensen (1973).

The $Q_d + Q_s$ separation was necessary to account for storage changes resulting from lags in soil and bedrock drainage (Kresic 1997). Hydrograph recessions were analyzed for a permanent gauge site further down the stream draining 168 ha that included the 16.6 ha study site. The recession analyses yielded discharge coefficients $\alpha_s = 0.26\ d^{-1}$ for shallow groundwater, and $\alpha_d = 0.12\ d^{-1}$ for deep groundwater, based on the linear reservoir exponential decay series:

$$Q(t) = Q_o e^{-\alpha t} \tag{5}$$

where Q(t) is daily base flow during zero runoff periods and $Q_0$ is the initial Q value for the series. For the 168 ha catchment of which this site is a sub-catchment, deep groundwater lags shallow drainage considerably – the same is assumed to apply for the study site (with different decay coefficients). It should be noted that $\alpha_s$ and $\alpha_d$ were not used to calculate the actual fluxes for the site, but rather to correct for inflows resulting from groundwater gradients extending up in the catchment being converted to shallow lateral flow. While this is a temporary condition following major events, it also occurs as seeps and springs that contribute to gauged runoff, $Q_r$. During events, such inflows are assumed to result from shallow groundwater flux, $Q_s$, produced by changes in soil moisture storage. The flow record was corrected such that long-term $\Sigma Q_s = 0$. Any further residual was attributed to $Q_d$.

Figure 3 shows the hydrological mass balance for the period 10 April 1996–26 March 1997 for which continuous runoff data were recorded at the site. Total precipitation at the site, 1.72 m, was the result of the wettest year on record. The effect of high precipitation on runoff is evident from the $Q_r$ curve. $Q_e$ behaves as expected. The $Q_d$ curve exhibits the long-term roughly linear loss expected, while $Q_s$ shows the daily fluctuation resulting from short-term changes induced by precipitation and drainage. The relatively low ratio of $Q_d$:$Q_r$ is typical for a headwater catchment, i.e., runoff volumes are high on steep slopes with shallow soil depth, and losses to groundwater are minimal by comparison.

*SRP mass balance*

Table 2 lists reported values for SRP (precipitation and groundwater values are included so that we can subsequently calculate the SRP mass balance). The SRP mass balance, with cumulative mass SRP export in runoff as shown in Figure 4, was constructed based on the hydrological mass balance. Runoff SRP concentrations were predicted by correlation analysis of 156 measured

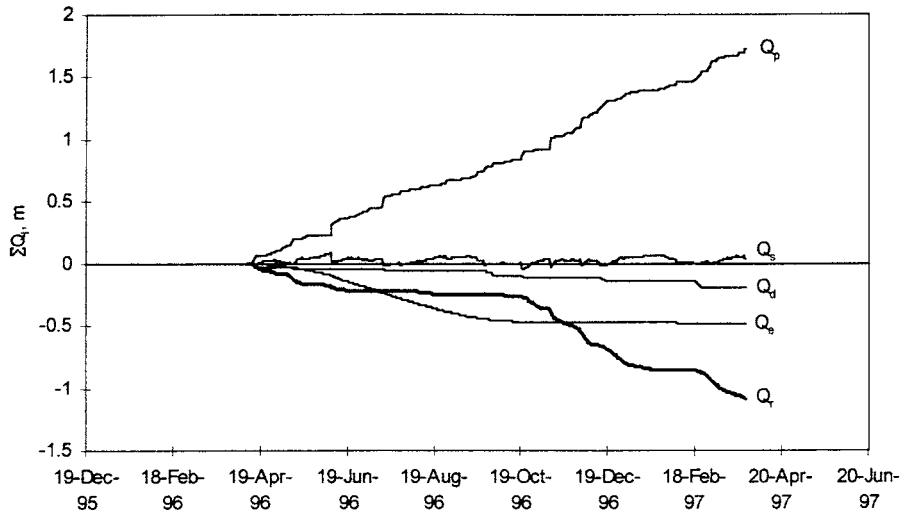


*Figure 3.* Hydrologic mass balance resulting from precipitation ($Q_p$), runoff ($Q_r$), evapotranspiration ($Q_e$), deep groundwater ($Q_d$), and soil moisture ($Q_s$) (all in units of [m], normalized by topographic contributing area).

SRP values as reported in Scott et al. (2001). SRP concentrations for the remaining flow components were as listed in Table 2. A constant deep groundwater $SRP_d$ concentration was calculated using the average $P_{available}$ value from Table 1 with the distribution coefficient for mineral soils reported above. The 0.0115 mg $L^{-1}$ result compares closely with the 0.013 mg $L^{-1}$ value reported in Haith et al. (1992). SRP in evapotranspiration was assumed zero. Precipitation $SRP_p$ values were taken from Zhang and Mitchell (1995). 0.002 mg $L^{-1}$ was used for the dormant season and 0.003 mg $L^{-1}$ for the growing season. Dry deposition of P was not considered in this study.

Cumulative SRP fluxes for the period of record are shown in Figure 5. The net SRP loss from the site was calculated as 0.118 kg $ha^{-1}$ for the period of record. Table 3 summarizes the annualized fluxes. It should be recalled that runoff in this study includes both surface flow and shallow lateral flow to the collection ditch which is approximately 1.5 m deep and collects some of the drainage leaching SRP from the surface litter to mineral soil horizons. Furthermore, the study period was a year of exceptionally high precipitation and flow volumes, resulting in the fluxes determined.

### *Model testing*

As indicated in the Methods section, we adapted the CSMR model to account for the spatial distribution of P source material as established by the assay.

*Table 2.* Reported SRP values for forest runoff, precipitation and groundwater

| Source | Forest Runoff SRP (mg $L^{-1}$) | Precipitation SRP (mg $L^{-1}$) | Groundwater SRP (mg $L^{-1}$) |
|---|---|---|---|
| Pekarova and Pekar (1996) | 0.01 | | |
| Likens and Bormann (1995) | 0.002 | 0.008 | |
| Zhang and Mitchell (1995) | | 0.002† | |
| | | 0.003‡ | |
| Haith et al. (1992) | 0.006 | | 0.013 |
| Yanai (1992) | | 0.0031§ | |
| Swank and Crossley (1988) | 0.006 | | |
| Likens (1985) | 0.0029 | 0.0097 | 0.005§ |
| Omernik (1977) | 0.006 | | |
| P. Longabucco, NYSDEC (1997, pers. communication) | 0.008 | | |

†dormant season.
‡growing season.
§calculated from data presented.

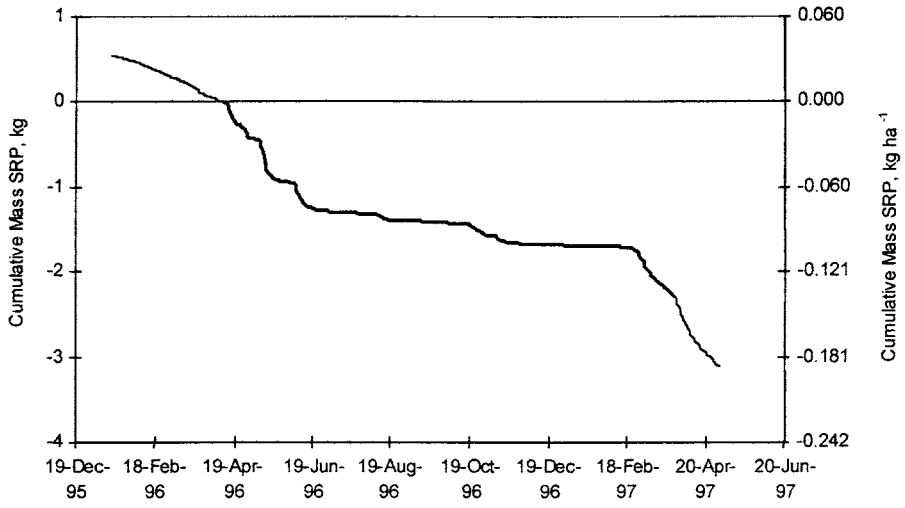


*Figure 4.* Cumulative SRP mass export in runoff (bold line using measured Q; standard line using simulated Q).

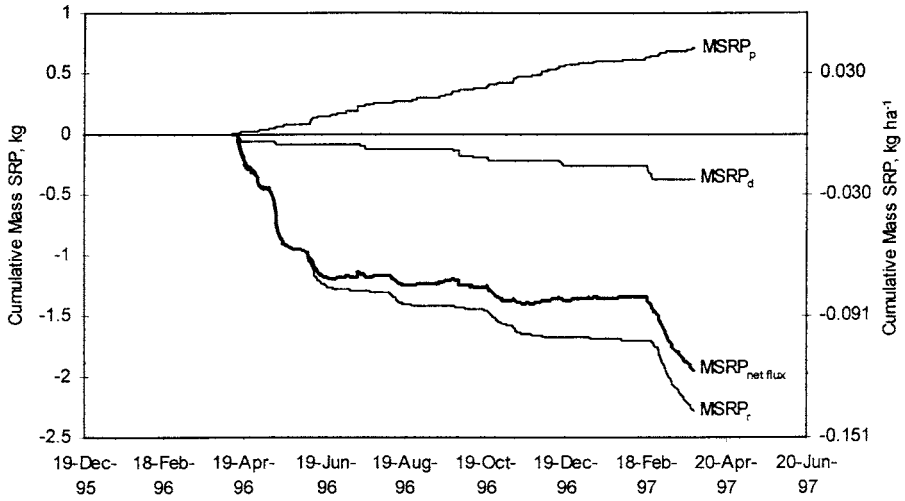


*Figure 5.* SRP mass balance showing net flux resulting from precipitation ($MSRP_p$), groundwater ($MSRP_d$), and runoff ($MSRP_r$).

*Table 3.* Annualized mass SRP fluxes

| | MSRP flux, kg $ha^{-1}$ $yr^{-1}$ |
|---|---|
| Net flux | –0.123 |
| Precipitation | 0.044 |
| Runoff | –0.143 |
| Groundwater | –0.024 |

The runoff volume generated on each cell was assumed to desorb available P in organic litter for that cell, according to the equilibrium relationship calculated using Equation 2 and the distribution coefficient $K_{d,litter}$. Figure 6 shows the contours of interpolated $P_{available}$ values for organic litter.

The simulated flow volume was 10% greater than the observed volume for the 10 April 1996–26 March 1997 period simulated. The model tended to over-predict both peaks and low flows with hydrograph recessions that were somewhat more rapid than observed (Figure 7). The difference between observed and simulated runoff during summer may be attributed to forest evapotranspiration that is simulated somewhat simplistically in the model. Additionally, rapid simulated hydrograph decline during fall and winter is simulated because snowmelt on frozen soils is not accounted for. It should be stressed that the model was developed to conceptually link hydrological and

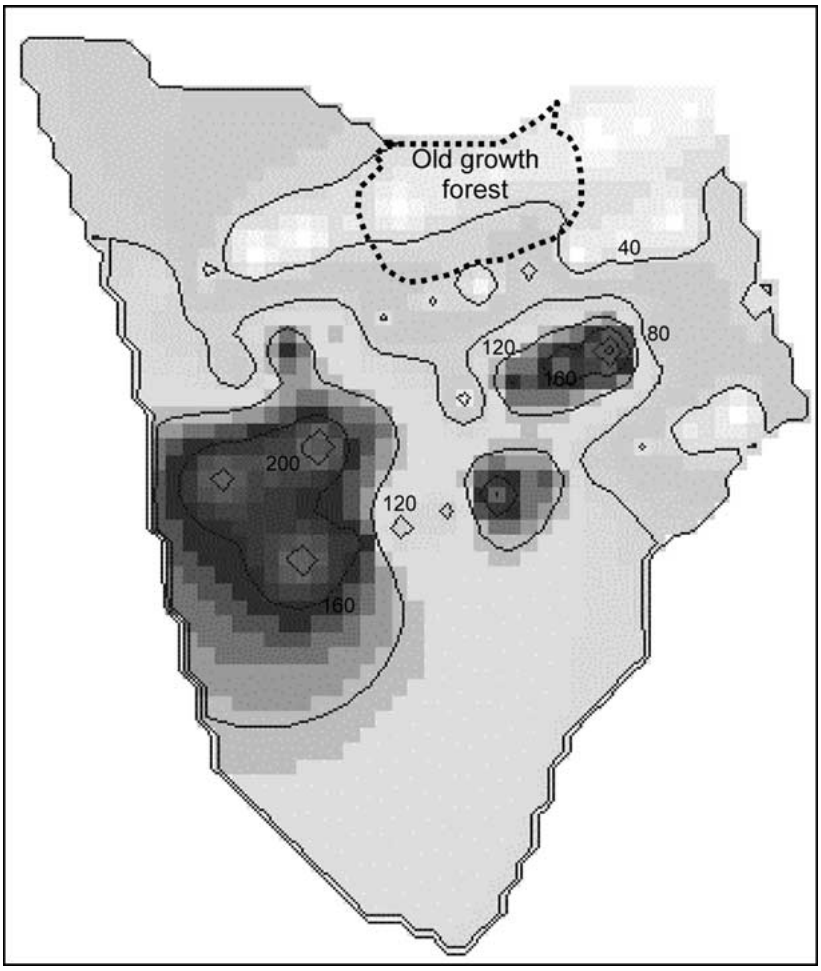


*Figure 6.* Interpolated surface of available P (mg $kg^{-1}$) in litter layer showing low values for old growth forest area.

biogeochemical processes and was not used to calculate the hydrological or SRP mass budgets presented above.

Based on the spatial distribution of P source material for runoff and the equilibrium concentrations for lateral flow and groundwater, the model output was used to calculate daily SRP time series proportionally weighted by the volume of each type of flow contributing to total outflow. These results are presented in Figure 8. The disparities between observed and simulated SRP concentrations indicate that desorption processes do not account for spring and summer SRP concentrations suggesting that other P release processes are

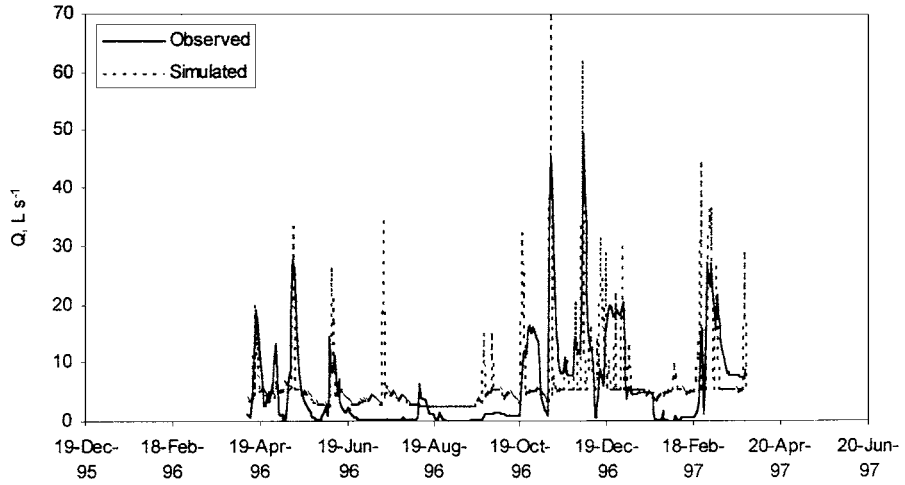


*Figure 7.* Observed and simulated runoff.

operative. Of particular interest is mineralization by aerobes during periods of low soil saturation.

## Conclusion

Hydrological and SRP mass balances based on field data from the successional forest site were constructed with annualized net SRP loss determined at 0.123 kg $ha^{-1}$ $yr^{-1}$. The elevated levels are attributed to residual P from historical farming practices. The results of this study differ significantly from the widely held view that forest ecosystems cycle P conservatively. Catchment ambient and equilibrium SRP concentrations were derived, corresponding to groundwater and long-term average runoff concentrations similar to $SRP_{mean}$ of 0.0127 mg $L^{-1}$. Further, observed and simulated SRP values suggest that concentrations are not explained by desorption processes alone. Given the extent of agricultural land abandonment in the northeastern U.S. and other regions, it likely that is this phenomenon is widespread. Although P export and eutrophication potential from land abanonment are currently lower than when more land was in agriculture, they are higher than for undisturbed, old-growth forest.

Based on estimated forest floor biomass of 65 T $ha^{-1}$ as dry weight (Yanai 1992), which includes only the $O_a$ horizon that is likely to have developed under regrowth forest, and a difference in available P content of 60 mg $kg^{-1}$ (from analysis of the data shown in Figure 6), there exists 5.1 kg $ha^{-1}$ of source P for the calculated SRP net loss. Conservatively, there appears to

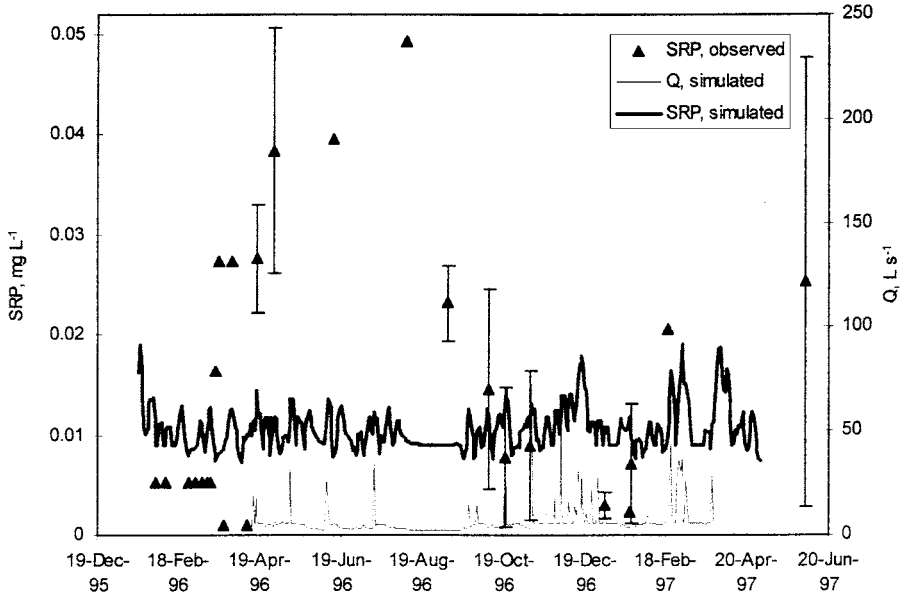


*Figure 8.* Observed and simulated SRP concentrations with simulated runoff.

be sufficient source material to sustain the calculated net SRP loss rate for at least another 30 years. The balance between P accumulation in biomass and hydrological export is site-specific; here, it is assumed that net loss will continue until P pools are diminished to levels at which accumulation just balances loss.

## Acknowledgements

The research reported on in this paper was supported by the Watershed Agricultural Council in Walton, New York, and the New York City Department of Environmental Protection.

## References

Boyer EW, Hornberger GM, Bencala KE & McKnight DM (1997) Response characteristics of DOC flushing in an alpine catchment. Hydrol. Proc. 11: 1635–1647

Dunne R & Black RD (1970) Partial area contributions to storm runoff in a small New England watershed. Water Resour. Res. 6: 1296–1311

Frankenberger JR, Brooks ES, Walter MT & Steenhuis TS (1999) A GIS-based variable source area model. Hydrol. Proc. 13(6): 804–822

Haith DA, Mandel R & Wu RS (1992) Generalized Watershed Loading Functions Version 2.0 User's Manual. Dept. Agricultural & Biological Engineering, Cornell University, Ithaca, NY

Hamon WR (1961) Estimating potential evapotranspiration. J. Hydraul. Div. Am. Soc. Civil Engr. May: 107–120.

Hewlett JD & Nutter WL (1970) The varying source area of streamflow from upland basins. In: Proceedings of the Symposium on Interdisciplinary Aspects of Watershed Management (pp 65–83). American Society of Civil Engineers, New York, NY

Jensen ME (Ed) (1973) Consumptive Use of Water and Irrigation Water Requirements (215 pp). American Society of Civil Engineers, New York, NY

Kresic N (1997) Quantitative Solutions in Hydrogeology and Groundwater Modeling. Lewis, Boca Raton, FL

Likens GE (1985) An Ecosystem Approach to Aquatic Ecology. Springer-Verlag, New York, NY

Likens GE & Bormann FH (1995) Biogeochemistry of a Forested Ecosystem. Springer-Verlag, New York, NY

Morgan MF (1941) Chemical soil diagnosis by the universal soil testing system. Conn. Agr. Exp. Sta. Bulletin 450

Omernik JM (1977) Nonpoint Source – Stream Nutrient Relationships: A Nationwide Study. EPA-600/3-77-105, Sept. 1977. Environmental Protection Agency, Corvallis, OR

Pekarova P & Pekar J (1996) The impact of land use on stream water quality in Slovakia. J. Hydrol. 80(1/4): 333–350

Rekolainen S (1989) Effect of snow and soil frost melting on the concentrations of suspended solids and phosphorus in two rural watersheds in western Finland. Aquat. Sci. 51(3): 211–223

Scott CA (1998a) The Hydrology of Phosphorus Transport in Watersheds of Mixed Agricultural and Forest Land Use. PhD dissertation. Cornell University, Ithaca, NY

Scott CA (1998b) Comment on 'Design for an inexpensive continuous digital output water level recorder' by S. Reedyk et al. (Paper 97WR00678). Water Resour. Res. 34(9): 2419–2421

Scott CA, Walter MF, Nagle GN, Walter MT, Sierra NV & Brooks ES (2001) Residual phosphorus in runoff from successional forest on abandoned agricultural land: 1. biogeochemical and hydrological processes. Biogeochem. 55: 293–309

Swank WT & Crossley DA Jr. (Eds) (1988) Forest Hydrology and Ecology at Coweeta. Springer-Verlag, New York, NY

Yanai RD (1992) Phosphorus budget of a 70-year-old northern hardwood forest. Biogeochem. 17: 1–22

Zhang Y & Mitchell MJ (1995) Phosphorus cycling in a hardwood forest in the Adirondack Mountains, New York. Can. J. For. Res. 25: 81–87

Zollweg JA, Gburek WJ & Steenhuis TS (1996) SMoRMod – a GIS-integrated rainfall-runoff model. Transactions ASAE. 39(4): 1299–1307